Heliyon 10 (2024) e24240

Contents lists available at ScienceDirect

Heliyon

journal homepage: www.cell.com/heliyon

Research article

# Sub-diffraction limited nanogroove fabrication of 30 nm features on diamond films using 800 nm femtosecond laser irradiation

Daqi Zhang , Tao Chen , Tianlun Shen , Yu Zhang , Yingsong He , Jinhai Si *, Xun Hou

*Key Laboratory of Physical Electronics and Devices, Ministry of Education and Shaanxi Key Laboratory of Information Photonic Technique, School of Electronic Science and Engineering, Xi'an Jiaotong University, No. 28, Xianning West Road, Xi'an, 710049, China*

ARTICLE INFO

*Keywords:*
LIPSS
Femtosecond laser
Nanofabrication
Diamond films
Sub-diffraction limited lithography

ABSTRACT

By controlling the 800 nm fs laser energy and applying an isopropyl alcohol environment, controlled sub-diffraction limited lithography with a characteristic structure of approximately 30 nm was achieved on the surface of diamond films, and diamond gratings with a period of 200 nm were fabricated. The fabrication of single grooves with a feature size of 30 nm demonstrates the potential for patterning periodic or nonperiodic structures, and the fabrication of 200 nm periodic grating structures demonstrates the ability of the technique to withstand laser proximity effects. This enhances the technology of diamond film nanofabrication and broadens its potential applications in areas such as optoelectronics and biology.

## 1. Introduction

The field of controlled nanofabrication forms a cornerstone of contemporary technological advancement and remains a persistent area of investigation within the scientific community. Compared to other nanofabrication methods, such as focused ion beam (FIB) [1], electron-beam lithography (EBL) [2,3], reactive ion etching (RIE) [4], and scanning probe lithography (SPL) [5], femtosecond laser nanoscale processing has the advantage of being easy to build, making it an attractive application in industrial manufacturing. However, the application of femtosecond lasers to high-resolution processing is hindered by the diffraction limit of the focused spot.

The use of laser-induced periodic surface structures (LIPSS) to overcome the diffraction limit in the preparation of nanogrooves has emerged as a cost-effective and convenient novel approach. The discovery of the LIPSS phenomenon is credited to Birnbaum, who first observed it in 1965 during the irradiation of semiconductor materials with a pulsed ruby laser [6]. Depending on the relationship between the spatial frequency and the wavelength of the irradiated laser, LIPSS structures are predominantly divided into two categories: low spatial frequency structures with a period similar to the utilized laser wavelength and high spatial frequency structures with a period significantly smaller than the wavelength. In theory, LIPSS structures can be prepared on all types of materials [7,8]. It has been demonstrated that low spatial frequency LIPSS (LSFL) can be implemented on a variety of materials, including metals, semiconductors, and dielectrics such as glasses, ceramics, and polymers [9–15]. High spatial frequency LIPSS (HSFL), characterized by a finer structure, was not discovered until the 1990s [16] and has been achieved on large-band-gap materials and several metals irradiated by ultrashort pulse lasers [9]. There is evidence to suggest that, when compared to air, liquid environments absorb laser radiation more readily [17,18], favoring the formation of HSFL and smaller feature sizes [19]. The production of large-area LIPSS structures on wide-band materials is common, and the principles of LIPSS formation are subject to a wide range of opinions. However,

* Corresponding author.
*E-mail address:* jinhaisi@mail.xjtu.edu.cn (J. Si).

https://doi.org/10.1016/j.heliyon.2024.e24240
Received 20 August 2023; Received in revised form 28 November 2023; Accepted 4 January 2024
Available online 9 January 2024

the heterogeneous nature of the LIPSS structure limits its technical application in many areas [20]. To prepare long-range ordered LIPSS structures, Huang et al. used the half-periodic mismatched optical enhancement (h-MOE) effect and a matched laser beam scanning strategy to prepare large-area controllable nanogrooves [21]. The optical far-field-induced near-field breakdown (O-FIB) technique based on the ripple effect has been proposed to obtain spatial resolutions of less than 20 nm on a variety of materials and relies on the generation of seed structures [22]. Additionally, through proper control of the laser fluence, precise control and preparation of a single nanogroove can be realized [23–25].

Diamond, owing to its superior physical and chemical properties, has a broad spectrum of applications across many fields. Synthetic diamonds, which mitigate the high cost of natural diamonds, offer extensive potential for application in electronics through the controlled growth and doping of chemical vapor deposition (CVD) diamonds [26]. Large-area LIPSS preparation on diamond using ultrashort pulsed lasers has been extensively studied [27–32]. Large sub 100 nm LIPSS structures were prepared on the upper surface of a diamond-like structure using HSFL and attributed to the excitation of short-range surface plasmon polaritons [33,34]. Large-area LIPSS structures have been produced in significant quantities by modifying laser parameters, allowing for expert attainment of their distinctive appearance and periodicity. Nevertheless, there is currently no method to create individual grooves on diamond film surfaces that would enable the production of a diverse range of nanostructure shapes, both periodic and nonperiodic.

In this work, a single groove with a width of 30 nm was achieved by direct irradiation on the diamond film surface using an 800 nm linearly polarized femtosecond laser, and a high linear density grating structure was formed by freely combining the groove points, demonstrating the high precision patterning capability of the femtosecond laser irradiation on the diamond film surface.

## 2. Experimental setup

As shown in Fig. 1(a)–a horizontally polarized femtosecond Gaussian laser beam with a central wavelength of 800 nm was generated by an amplified Ti: sapphire laser (Libra-USP-HE, Coherent, USA). The laser radiation had a pulse frequency of 1 kHz and an energy output of 3.5 mJ. The beam was modulated by a PC-operated high-speed shutter (HF200HT, Prior, 10 ms) and attenuated by an adjustable attenuator. The diaphragm was adjusted to a 5 mm size to select the center portion of the laser beam and simultaneously guarantee that the aperture of the objective lens (4 mm) was filled full by the laser beam. The beam was then directed to a high-precision microprocessing stage and focused on the sample surface by an objective lens (Nikon LU Plan Fluor 100×, NA0.9). The focal spot size $\omega$ is defined by the numerical aperture ($NA$) of the focusing lens and wavelength, $\lambda$, as $\omega = 1.22\lambda/NA$ [35]. Under optimal conditions, the spot produced by focusing through the 100× objective lens is determined to be 1084 nm due to the diffraction limit.

The samples were placed on a three-dimensional carrier platform with high precision. The platform, driven by a ProScan III Controller, had a repeatability of ±0.15 μm and a minimum step interval of 50 nm. The samples consisted of Microcrystalline Diamond (MCD) layers with a thickness of 450 nm and a boron doping concentration of 500 ppm. The MCD layers were grown on silicon wafers with a thickness of 500 μm and a (100) orientation by the Hot Filament Vapor Deposition (HFCVD) technique from NeoCoat. The samples had a surface roughness ranging from 10 nm to 15 nm. Diamond film samples were submerged in an isopropyl alcohol (IPA) 99 % solution that was contained within a glass Petri dish. To decrease the volatilization of the IPA, a coverslip (Matsunami NEO NO.1) was positioned on top of the diamond film, as shown in Fig. 1(b). The thickness of the IPA liquid bridge formed on the diamond film

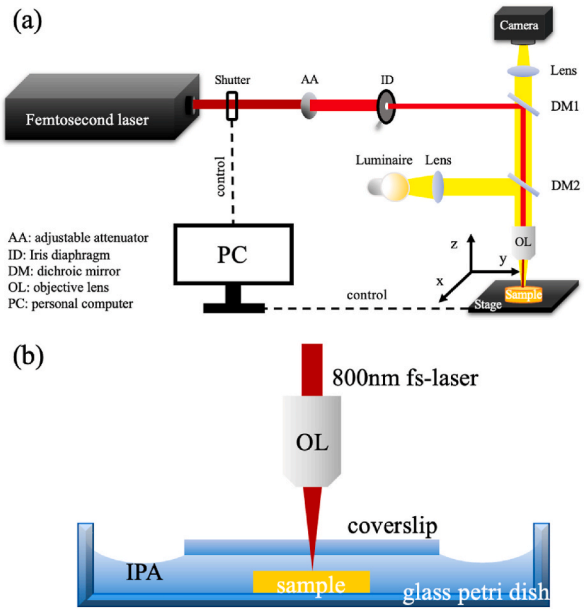


**Fig. 1.** Schematic diagram of the femtosecond laser precision machining system. (a) System as a whole (b) Sample environment.

surface and under the coverslip was approximately 2 μm. The IPA in the Petri dish provided a constant supply of IPA on the diamond film, ensuring stability during processing. It should be noted that the IPA used in the Petri dish must not exceed the microscope coverslip. All scanning speeds are set at 10 μm/s.

Note that laser energy is lost through reflections from multiple medium boundaries. And losses due to multiphoton absorption of the laser energy in the IPA are not negligible [36], so the energy deposited on the surface of the diamond film is not accurate at this time, whereas the energy measured behind the aperture can be relatively sensitive to the current laser energy settings. As the laser beam passes through two dichroic mirrors the energy measured value is reduced to one-quarter of the laser energy that eventually enters the objective lens. The energy density of the laser radiation can be derived from the following equation:

$$\varphi = \frac{4P}{f_{rep}\pi\omega^2}$$

where $\varphi$ is the laser energy density, $P$ is the average laser power, which is one-quarter of the measured laser power, $\omega$ is the laser beam diameter after focusing, and $f_{rep}$ is the laser repetition frequency.

Nanostructures in the exposed area were observed by a Zeiss Gemini SEM500 Field Emission Scanning Electron Microscopy (SEM) and a Veeco Innova Atomic Force Microscope (AFM), and the widths were determined using SEM images in combination with an imaging software tool.

## 3. Results

Fig. 2(a) demonstrates the uniform distribution of micron-sized diamond particles on the surface of the unirradiated diamond. As seen in Fig. 2(b), at a laser energy density of 3.3 J/cm$^2$, which is above the damage threshold of the diamond film, a single scan can prepare a single continuous groove structure with a width of approximately 30 nm, much smaller than the diffraction limit, but surrounded by laser irradiation damage and fine debris. The results of multiple scans are shown in Fig. 2(c). Under the same conditions as in Fig. 2(b), when multiple scans are performed on a diamond film with an interval of 200 nm between each scan, a large amount of processing debris, which cannot be cleaned by ultrasonic waves, is generated during the preparation process and accumulates with the increase in the number of scans, resulting in a part of the area that cannot be irradiated effectively by the laser, and a discontinuous structure with poor quality is prepared. Fig. 2(d) illustrates that when using the IPA setup, three parallel nanogrooves appear with a fixed period of approximately 200 nm per scan as soon as the laser energy exceeds the energy used for individual trench preparation, as demonstrated in Fig. 3. This is typical of HSFL ($\Lambda \leq \lambda/4$). When the laser energy decreases to the results shown in Fig. 3, no structure is created on the film surface.

Contrary to direct laser irradiation in the air, diamond grains near the nanogroove showed remarkable preservation and minimal collateral damage when processed in an IPA environment. As demonstrated in Fig. 3(a) and (b), a unique structure, approximately 30 nm wide, was visible on the diamond film surface without any apparent deposition of processing debris.

The presence of the proximity effect causes the first structure fabricated during nanofabrication to affect the fabrication of subsequent structures, especially when the second feature is close to the first [37]. To challenge this technique's resilience in the face of proximity effects, Fig. 3(c) depicts the experimental outcomes when conducting a laser beam scan with a lateral pitch of 200 nm. The well-defined 200 nm grating period and approximately 30 nm groove width demonstrate this method's resilience against laser proximity effects and potential for high-density nanogroove fabrication. Graphitization of diamonds is an inevitable consequence of femtosecond laser irradiation. Unlike the direct irradiation of diamonds by a femtosecond laser in the air, which is demonstrated in Fig. 2(c), the accumulation of graphite fragments has a negative impact on normal processing. Conversely, the application of an IPA environment resulted in a consistently stable and clean environment during processing, which allowed us to achieve the preparation of grating structures with a pitch of 200 nm and no further treatment to make the structures clean.

Fig. 3(d), (e), and (f) illustrate the impact of laser irradiation on the diamond film during the platform's acceleration, deceleration, and steady-speed phases, respectively. During acceleration and deceleration, collateral streak-like damage was noticeable around the main structure on the diamond film surface. In contrast, if the shutter controlled by software is closed during the steady-speed phase, only a distinct groove parallel to the scanning direction appears. This means that arbitrary writing of completely single grooves is easily achieved by good coordination of the stage and the shutter. These results imply that the creation of a single controllable structure

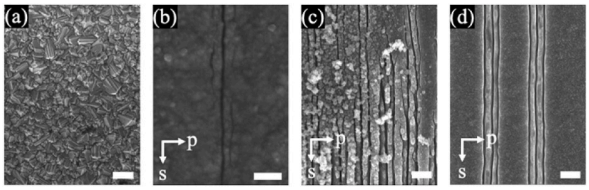


**Fig. 2.** SEM images of the diamond film and surface LIPSS structure; all scales in the figure are 400 nm, s: scanning direction, p: polarization direction. (a) Original state of the diamond film (b) Irradiation result of a single scan of a femtosecond laser at a power near the diamond destruction threshold (laser power measured at 120 μW), air environment (c) Irradiation result of multiple scans of a femtosecond laser at a power near the diamond destruction threshold with an interval of 200 nm per scan, air environment (d) When the laser energy is greater (measured at 650 μW) than the nanogrooves shown in Fig. 3, the IPA environment, two scans of the same conditioned laser in separate regions.

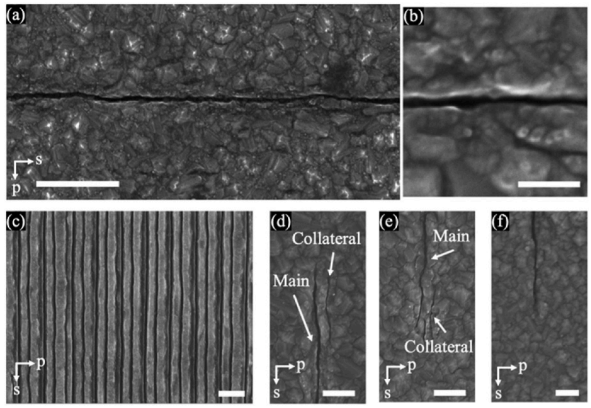


**Fig. 3.** Sub-diffraction limited lithography SEM image of the diamond film surface, all scales in the figure are 400 nm, except in figure (a) where the scale is 1 μm, s: scanning direction, p: polarization direction, laser power measured at 600 μW. (a) Single groove on the surface of the diamond film (b) Enlarged view of single groove (c) Diamond grating with a period of 200 nm, displayed directly after laser treatment, no further treatment has been applied (d) Laser irradiation results in the initial acceleration stage of the platform (e) Laser irradiation results in the final deceleration stage of the platform (f) Result when the shutter is closed while the platform is running at a constant speed.

requires a uniform distribution of laser energy deposition.

Notably, under laser energy conditions that could produce a single nanogroove, no nanogroove appeared on the diamond films when the scanning direction was changed to coincide with the laser polarization direction, highlighting the importance of the relationship between polarization and scanning direction for consistency in the fabrication of diamond film nanogrooves.

AFM results obtained from sub-diffraction limit lithography performed on the surface of a diamond film, as illustrated in Fig. 4, indicate that the grains on the MCD film measured approximately 80 nm in height and had a baseline. The diamond's ultra-high hardness makes it easy to damage the AFM tip. When the tip is damaged, it produces a typical fake feature located beside the grooves, shown in Fig. 4(b). This fake feature severely affects our judgment of the groove's width and can be easily confused, particularly at this scale. The intricate arrangement of diamond particles notwithstanding, the amalgamation of the AFM grooves' partial results with the more detailed SEM outcomes established the existence of a distinctive configuration with a width of 34 nm in the laser-irradiated film section. Irregular surface patterns and the haphazard distribution of grain boundaries impact the polarization of the laser, causing the formation of warped grooves.

Fig. 5 illustrates the statistical analysis of the individual nanogroove widths shown in Fig. 3(b). The widths are distributed in a Gaussian fashion, with the maximum likelihood at 22.5 nm. In addition, in this section of the groove, the average width achieves 28 nm, which corroborates the efficacy of the technique to attain sub-30 nm level fabrication on the surface of diamond film. The nanogroove's width variability may be attributed to the instability of the laser radiation output power. This phenomenon occurs more often in the search for extreme processing resolution and even small perturbations are amplified by nonlinear effects.

## 4. Discussion & conclusions

While the threshold effect has permitted femtosecond laser applications in subwavelength etching of different materials, applying

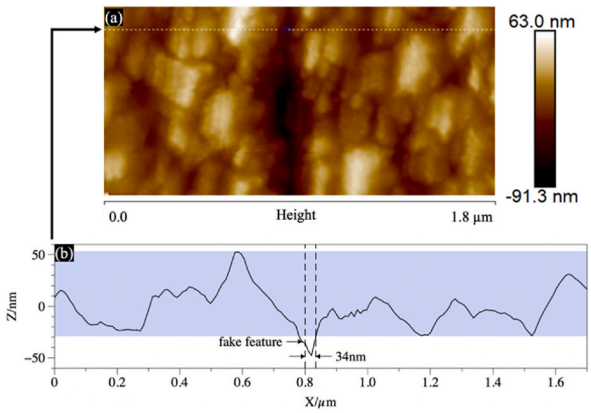


**Fig. 4.** AFM results of sub-diffraction limited lithography on the surface of diamond films. (a) 2D geometrical topography (b) Height contour map perpendicular to the laser beam scanning direction, marked by the white dashed line in (a).

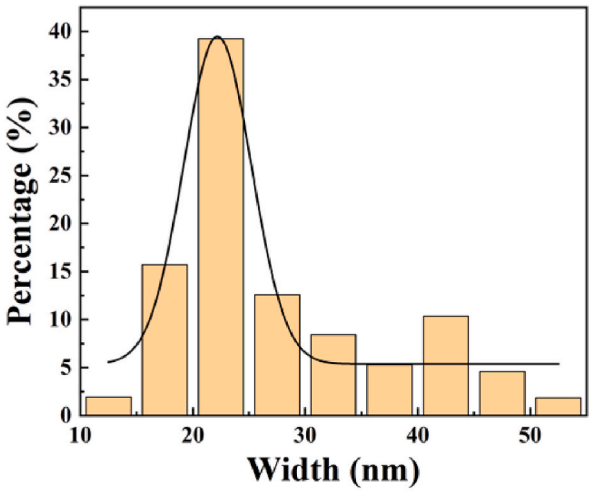


**Fig. 5.** Statistical analysis of single groove width.

femtosecond lasers to prepare nanogrooves is often challenging due to multiple factors that hinder easy, high-quality, and controlled operations. Direct irradiation of the diamond film with femtosecond lasers in an air environment frequently leads to fragmentation and collateral damage, profoundly impacting the preparation quality. The dominance of the LIPSS effect in the formation of nanogrooves is proven by the energy sensitivity and polarization sensitivity demonstrated by these results. Additionally, the period and structural features confirm that the HSFL effect in LIPSS is responsible for the results presented in this work. The application of a liquid environment carries away most of the ablated material and spare heat generated during the laser ablation process, avoiding the impact of debris on subsequent laser energy deposition [24,38]. While both water and methanol can remove debris from the process at the same fast rate, sub-diffraction limit lithography results have not been seen due to their greater tendency to create bubbles that interfere with the laser irradiation process. For diamond films, the IPA environment is more stable while taking away debris from the processed surface, providing a reliable environment for subsequent processing, and is key to achieving the sub-diffraction limited lithography. The formation of single sub-30 nm nanogroove is attributed to the interaction between the laser pulse and the laser-induced plasma, as well as appropriate laser energy control. Based on fundamental plasmonic theories, scaling-down occurs spontaneously due to the conversion of physical regimes of plasmonic interaction from the optical regime to the electrostatic regime. This triggers the generation of quasistatic surface plasmons with interaction scales far beyond the diffraction limit resulting in enhanced electrostatic fields [39]. The application of a liquid environment with the IPA allows the incident laser fluence and laser-induced plasma interference to be stably generated in the region of the enhanced electrostatic field, an advantage that is difficult to achieve in an air environment. This ultrafast nonthermal formation process also has the ability to withstand laser proximity effects, allowing for the creation of nanostructures with higher density. However, the physical mechanism behind the formation of single sub-30 nm nanogroove is highly intricate and necessitates further investigation. As such, the fabrication of nanogroove on diamond surfaces becomes more feasible and promising, signaling a bright future for this advanced manufacturing technique.

This study presents a significant advancement in fabricating individual nanogroove on diamond films, allowing the controlled and easy production of individual nanogroove of better quality and with a resistance to proximity effects of at least 200 nm. The diamond film is a material that possesses special properties and presents significant processing challenges. Individual diamond grooves at the 30 nm level can significantly impact the optical, electrical, and mechanical properties of diamond films, leading to various applications. Thanks to the utilization of femtosecond laser processing in an IPA environment, this research has surmounted the previous challenges, including diffraction limits and collateral damage. Accomplishing precise features of 30 nm under control underscores the potential this technology offers, particularly in the semiconductor fabrication industry. Consequently, with the application of an IPA environment, sub-30 nm diamond film surface features can be prepared using an 800 nm fs laser, enabling independent formation and even a free pattern on the diamond surface, such as a 200 nm grating structure, which not only enriches the diamond nanofabrication technology but also greatly expands the prospects and possibilities for the application of diamond films, particularly in the areas of nanophotonics and optoelectronic devices in extreme conditions, and for sensing, detecting, and other biological applications where diamond demonstrates exceptional performance.

## Funding

National Key Research and Development Program of China under Grant 2019YFA0706402HZ; National Natural Science Foundation of China under Grants 62,027,822.

## Data availability statement

Data will be made available on request.

## Additional information

No additional information is available for this paper.

## CRediT authorship contribution statement

**Daqi Zhang:** Writing – review & editing, Writing – original draft, Visualization, Validation, Methodology, Investigation, Formal analysis, Data curation, Conceptualization. **Tao Chen:** Writing – review & editing, Supervision, Methodology, Investigation, Formal analysis, Conceptualization. **Tianlun Shen:** Validation, Supervision, Data curation. **Yu Zhang:** Validation, Software, Data curation. **Yingsong He:** Validation, Software, Investigation, Data curation. **Jinhai Si:** Writing – review & editing, Supervision, Resources, Project administration, Methodology, Formal analysis. **Xun Hou:** Supervision, Resources, Methodology, Funding acquisition.

## Declaration of competing interest

The authors declare that they have no known competing financial interests or personal relationships that could have appeared to influence the work reported in this paper.

## Acknowledgment

The characterization of this work was supported by the Instrumental Analysis Center of Xi'an Jiaotong University and its staff, Mr. Fan Haitao.

## References

[1] P. Li, S. Chen, H. Dai, Z. Yang, Z. Chen, Y. Wang, Y. Chen, W. Peng, W. Shan, H. Duan, Recent advances in focused ion beam nanofabrication for nanostructures and devices: fundamentals and applications, Nanoscale 13 (2021) 1529–1565.
[2] C. Vieu, F. Carcenac, A. Pépin, Y. Chen, M. Mejias, A. Lebib, L. Manin-Ferlazzo, L. Couraud, H. Launois, Electron beam lithography: resolution limits and applications, Appl. Surf. Sci. 164 (2000) 111–117.
[3] J.N. Randall, J.H.G. Owen, J. Lake, E. Fuchs, Next generation of extreme-resolution electron beam lithography, J. Vac. Sci. Technol. B 37 (2019) 061605.
[4] S.-C. Shin, T. Park, J.-Y. Baek, S. Kim, J.-S. Kwon, M. Hong, K. Nam, C. Lim, S. Oh, S. Cho, K.-K. Kim, SiO $_2$/ITO nanostructure fabricated by nano-lithography using a self-arrayed colloidal monolayer, J. Nanosci. Nanotechnol. 17 (2017) 7869–7873.
[5] K. Xu, J. Chen, High-resolution scanning probe lithography technology: a review, Appl. Nanosci. 10 (2020) 1013–1022.
[6] M. Birnbaum, Semiconductor surface damage produced by ruby lasers, J. Appl. Phys. 36 (1965) 3688–3689.
[7] Y. Zhang, Q. Jiang, M. Long, R. Han, K. Cao, S. Zhang, D. Feng, T. Jia, Z. Sun, J. Qiu, H. Xu, Femtosecond laser-induced periodic structures: mechanisms, techniques, and applications, OES 1 (2022) 220005–220021.
[8] D. Zhang, R. Liu, Z. Li, Irregular LIPSS produced on metals by single linearly polarized femtosecond laser, Int. J. Extrem. Manuf. 4 (2021) 015102.
[9] J. Bonse, J. Krüger, S. Höhm, A. Rosenfeld, Femtosecond laser-induced periodic surface structures, J. Laser Appl. 24 (2012) 042006.
[10] C. Kunz, J.F. Bartolomé, E. Gnecco, F.A. Müller, S. Gräf, Selective generation of laser-induced periodic surface structures on Al2O3-ZrO2-Nb composites, Appl. Surf. Sci. 434 (2018) 582–587.
[11] C. Kunz, J. Bonse, D. Spaltmann, C. Neumann, A. Turchanin, J.F. Bartolomé, F.A. Müller, S. Gräf, Tribological performance of metal-reinforced ceramic composites selectively structured with femtosecond laser-induced periodic surface structures, Appl. Surf. Sci. 499 (2020) 143917.
[12] A. Rodríguez, M.C. Morant-Miñana, A. Dias-Ponte, M. Martínez-Calderón, M. Gómez-Aranzadi, S.M. Olaizola, Femtosecond laser-induced periodic surface nanostructuring of sputtered platinum thin films, Appl. Surf. Sci. 351 (2015) 135–139.
[13] P. Nürnberger, H.M. Reinhardt, H.-C. Kim, E. Pfeifer, M. Kroll, S. Müller, F. Yang, N.A. Hampp, Orthogonally superimposed laser-induced periodic surface structures (LIPSS) upon nanosecond laser pulse irradiation of SiO2/Si layered systems, Appl. Surf. Sci. 425 (2017) 682–688.
[14] M. Kasischke, S. Maragkaki, S. Volz, A. Ostendorf, E.L. Gurevich, Simultaneous nanopatterning and reduction of graphene oxide by femtosecond laser pulses, Appl. Surf. Sci. 445 (2018) 197–203.
[15] T. Zou, B. Zhao, W. Xin, Y. Wang, B. Wang, X. Zheng, H. Xie, Z. Zhang, J. Yang, C. Guo, High-speed femtosecond laser plasmonic lithography and reduction of graphene oxide for anisotropic photoresponse, Light Sci. Appl. 9 (2020) 69.
[16] J. Heitz, E. Arenholz, D. Bäuerle, R. Sauerbrey, H.M. Phillips, Femtosecond excimer-laser-induced structure formation on polymers, Appl. Phys. A 59 (1994) 289–293.
[17] D. Zhang, K. Sugioka, Hierarchical microstructures with high spatial frequency laser induced periodic surface structures possessing different orientations created by femtosecond laser ablation of silicon in liquids, OEA 2 (2019) 190002–190018.
[18] D. Zhang, B. Ranjan, T. Tanaka, K. Sugioka, Underwater persistent bubble-assisted femtosecond laser ablation for hierarchical micro/nanostructuring, Int. J. Extrem. Manuf. 2 (2020) 015001.
[19] D. Zhang, B. Gökce, S. Sommer, R. Streubel, S. Barcikowski, Debris-free rear-side picosecond laser ablation of thin germanium wafers in water with ethanol, Appl. Surf. Sci. 367 (2016) 222–230.
[20] J. Huang, K. Xu, S. Xu, X. Li, Q. Wei, Self-aligned laser-induced periodic surface structures for large-area controllable nanopatterning, Laser Photon. Rev. 16 (2022) 2200093.
[21] J. Huang, K. Xu, J. Hu, D. Yuan, J. Li, J. Qiao, S. Xu, Self-aligned plasmonic lithography for maskless fabrication of large-area long-range ordered 2D nanostructures, Nano Lett. 22 (2022) 6223–6228.
[22] Z.-Z. Li, L. Wang, H. Fan, Y.-H. Yu, Q.-D. Chen, S. Juodkazis, H.-B. Sun, O-FIB: far-field-induced near-field breakdown for direct nanowriting in an atmospheric environment, Light Sci. Appl. 9 (2020) 41.
[23] R. Taylor, C. Hnatovsky, E. Simova, Applications of femtosecond laser induced self-organized planar nanocracks inside fused silica glass, Laser Photon. Rev. 2 (2008) 26–46.
[24] J. Liu, T. Jia, K. Zhou, D. Feng, S. Zhang, H. Zhang, X. Jia, Z. Sun, J. Qiu, Direct writing of 150 nm gratings and squares on ZnO crystal in water by using 800 nm femtosecond laser, Opt Express 22 (2014) 32361.

[25] X. He, A. Datta, W. Nam, L.M. Traverso, X. Xu, Sub-diffraction limited writing based on laser induced periodic surface structures (LIPSS), Sci. Rep. 6 (2016) 35035.
[26] A. Gicquel, K. Hassouni, F. Silva, J. Achard, CVD diamond films: from growth to applications, Curr. Appl. Phys. 1 (2001) 479–496.
[27] P. Calvani, A. Bellucci, M. Girolami, S. Orlando, V. Valentini, A. Lettino, D.M. Trucchi, Optical properties of femtosecond laser-treated diamond, Appl. Phys. A 117 (2014) 25–29.
[28] D.M. Trucchi, A. Bellucci, M. Girolami, M. Mastellone, S. Orlando, Surface texturing of CVD diamond assisted by ultrashort laser pulses, Coatings 7 (2017) 185.
[29] A.F. Sartori, S. Orlando, A. Bellucci, D.M. Trucchi, S. Abrahami, T. Boehme, T. Hantschel, W. Vandervorst, J.G. Buijnsters, Laser-induced periodic surface structures (LIPSS) on heavily boron-doped diamond for electrode applications, ACS Appl. Mater. Interfaces 10 (2018) 43236–43251.
[30] M. Mastellone, A. Bellucci, M. Girolami, V. Serpente, R. Polini, S. Orlando, A. Santagata, E. Sani, F. Hitzel, D.M. Trucchi, Deep-subwavelength 2D periodic surface nanostructures on diamond by double-pulse femtosecond laser irradiation, Nano Lett. 21 (2021) 4477–4483.
[31] M. Mastellone, M.L. Pace, M. Curcio, N. Caggiano, A. De Bonis, R. Teghil, P. Dolce, D. Mollica, S. Orlando, A. Santagata, V. Serpente, A. Bellucci, M. Girolami, R. Polini, D.M. Trucchi, LIPSS applied to wide bandgap semiconductors and dielectrics: assessment and future perspectives, Materials 15 (2022) 1378.
[32] M. Mastellone, E. Bolli, V. Valentini, S. Orlando, A. Lettino, R. Polini, J.G. Buijnsters, A. Bellucci, D.M. Trucchi, Surface nanotexturing of boron-doped diamond films by ultrashort laser pulses, Micromachines 14 (2023) 389.
[33] S.M. Pimenov, E.V. Zavedeev, N.R. Arutyunyan, B. Jaeggi, B. Neuenschwander, Femtosecond laser-induced periodic surface structures on diamond-like nanocomposite films, Diam. Relat. Mater. 130 (2022) 109517.
[34] Y. Iida, S. Nikaido, G. Miyaji, Sub-100-nm periodic nanostructure formation induced by short-range surface plasmon polaritons excited with few-cycle laser pulses, J. Appl. Phys. 130 (2021) 183102.
[35] M. Malinauskas, M. Farsari, A. Piskarskas, S. Juodkazis, Ultrafast laser nanostructuring of photopolymers: a decade of advances, Phys. Rep. 533 (2013) 1–31.
[36] D. Zhang, B. Gökce, S. Barcikowski, Laser synthesis and processing of colloids: fundamentals and applications, Chem. Rev. 117 (2017) 3990–4103.
[37] C. Arnoux, L.A. Pérez-Covarrubias, A. Khaldi, Q. Carlier, P.L. Baldeck, K. Heggarty, A. Banyasz, C. Monnereau, Understanding and overcoming proximity effects in multi-spot two-photon direct laser writing, Addit. Manuf. 49 (2022) 102491.
[38] A.P. Joglekar, H. Liu, E. Meyhöfer, G. Mourou, A.J. Hunt, Optics at critical intensity: applications to nanomorphing, Proc. Natl. Acad. Sci. U.S.A. 101 (2004) 5856–5861.
[39] M. Huang, Z. Xu, Spontaneous scaling down of femtosecond laser-induced apertures towards the 10-nanometer level: the excitation of quasistatic surface plasmons, Laser Photon. Rev. 8 (2014) 633–652.